Application of the PTVA–4 Modeling in Assessment of Building Vulnerability to Earthquake and Tsunami: A Simple and Reliable Method for Preliminary Study of Tsunami-Prone Zones

*[1,2]FX Anjar Tri Laksono and [1]János Kovács
*[1]The Doctoral School of Earth Sciences, Department of Geology and Meteorology, Institute of Geography and Earth Sciences, Faculty of Sciences, University of Pécs, H-7624, Ifjúsag str. 6, Pécs, Baranya, Hungary
[2]The Department of Geological Engineering, Faculty of Engineering, Jenderal Soedirman University, 53371, Purbalingga, Central Java, Indonesia

Abstract

The earthquake and tsunami in Aceh Province, Indonesia, in 2004 caused the deaths of nearly 200,000 people and an economic loss of up to USD 4 billion. The recurrence period for the tsunami in Aceh is 250-400 years. Along the subduction zone between the Eurasia continental plate and the Indo-Australia oceanic plate, the southern region of Java Island is a vulnerable zone whose recurrence period is not known until nowadays. This zone is a densely populated area and the largest source of Indonesian economic income besides the north coast of Java. Therefore, a building vulnerability study is needed to minimize casualties and financial losses. The PTVA–4 modeling is a suitable method to be developed because it is reliable and does not require high costs. We conclude that this method is accurate by assessing the modelling results on the impact of the 2006 earthquake and tsunami in Cilacap, Indonesia.

Key words: PTVA–4, building vulnerability, subduction zone, earthquake, tsunami

1. Introduction

In the last ten years, the tsunami disaster has resulted in more than 200 thousand people dying, hundreds of thousands of houses devastated, thousands of public infrastructure destroyed, and economic losses were reaching more than 10 billion USD [1,2]. Almost all tsunami events that occur in the world begin with an earthquake [3,4]. However, tsunamis are not only generated by tectonic earthquakes due to collisions or plate shifts, meteorites falling into the sea, underwater volcanic eruptions, and submarine landslides that can induce tsunamis [5,6]. An example of a tsunami event caused by a volcanic eruption is the 2018 tsunami in Anyer Beach, Indonesia [7]. Anak Krakatau erupted and caused an underwater avalanche. In 1883, the eruption of Mount Krakatau also caused large sea waves to separate the island of Java from Sumatra [8]. The tsunami caused by tectonics occurred in Aceh in 2004, Pangandaran and Cilacap in 2006, Lombok and Palu in 2018. Even the Palu earthquake and tsunami in 2018 were followed by a liquefaction disaster that generated buildings to collapse and be buried underground [9]. A tectonic earthquake that caused a tsunami also occurred in Tohoku, Japan, in 2011, followed by the Fukushima nuclear disaster [10,11]. In 2022, a tsunami was due to a volcanic eruption near the Tonga region that killed thousands of people. The height of this tsunami wave reached 15 meters on Tongatapu Island.

Most of the deaths from the earthquake and tsunami are caused by being buried under the rubble of buildings [12]. The victims are trapped inside buildings and unable to evacuate themselves during the earthquake. The next cause of death was that the victims were carried away by the

current of the tsunami waves, which had high speed [13]. Hence they had no chance to escape. In the earthquake and tsunami mitigation studies, there are two crucial factors to minimise casualties and economic losses, namely the resilience of the building and the distance of the building from the shoreline [14,15]. This chapter will explain the assessment of the vulnerability of buildings to earthquakes and tsunamis using PTVA–4 modeling. To facilitate understanding of this modeling, an example of the PTVA–4 application on the southern coast of Cilacap, Central Java, Indonesia, will be given. A tsunami struck this location in 2006, which killed 664 people and caused 1623 houses destruction [16–18]. The potential for earthquakes and tsunamis in the future is still very high because this area is only about 500 km from the epicenter of the subduction zone earthquake between the Eurasian and Indo-Australian plates [19]. Many earthquake epicenter points are currently unknown. A small part of the earthquake's epicenter has released energy that causes earthquakes above Mw 5. Nevertheless, most of the existing epicenters have not caused an earthquake in the last 100 years. The most feared in the southern java subduction zone is that the significant accumulation of energy in the seismic gap will trigger a high magnitude and destructive earthquake [20,21].

2. Materials and Method

Tsunami inundation modeling can be created using ArcGIS 10.8.1 software with the output of PTVA–4 (Papathoma Tsunami Vulnerability Assessment). The PTVA–4 is modeling using building parameters as a measuring object to determine the vulnerability of the building to tsunami events by assigning a score in the form of a Relative Vulnerability Index (RVI) for each building by considering certain factors such as Structural Vulnerability (SV) and building resilience due to contact with water during the tsunami process (WV). The calculation of the RVI score is determined from the SV and WV components, using the formula 1 [22]:

$$RVI = \frac{2}{3}\,(SV) + \frac{1}{3}\,(WV) \qquad (1)$$

Where:
RVI = Relative Vulnerability Index
SV = Structure Vulnerability
WV = Building resistance to inundation
The SV component of each building is determined based on attributes encompassing the building structure level (BV), surrounding protection (Surr), and the building location against water depth existence (Ex). The value of SV can be sought by equation 2 [23]:

$$SV = BV.Surr.Ex \qquad (2)$$

The value of BV is based on the following parameters: the floor number of the building (s), building material (m), ground floor openness (g), foundation depth (f), building structural form (sh), and the maintenance condition of the building (pc) (**Table 1**). Entire these components input into the equation 3 [24]:

$$v = 1/409\ (100(m) + 85(s) + 69.(g) + 69(f) + 52(sh) + 34(pc)) \qquad (3)$$

Surr components overwhelm the number of natural barriers (nb), rows of surrounding buildings (br), the presence of seawalls (sw), surrounding building walls (n), and the risk of moving objects (mo) (**Table 2**) (equation 4) [25]:

$$Surr = 1/356\,(100(br) + 84(sw) + 72(nb) + 58(mo) + 42(w)) \qquad (4)$$

The water depth determines the exposure value against the building. The score is based on the

water depth above the terrain level (Wd) with the maximum water depth (Wdmax) (equation 5) [26].

$$Ex = \frac{Wd}{Wd_{max}} \qquad (5)$$

Table 1. Score attribute on the building structure level components [24,26]

Components	-1	-0.5	0	+0.5	+1
The number of floor (s)	More than five floors	Four floors	Three floor	Two floors	One floor
Building material (m)	Reinforced concrete or steel		Brick		Wood, tin, clay, or other lightweight materials
Ground floor hydrodynamics (g)	Outdoor	About 75% open space	About 50% open space	About 25% open space	No open space, very few open spaces on the ground floor
Foundation resistance (f)	Deep pile foundation		Foundation with average depth		Shallow foundation
Building footprint (sh)	Circles or triangles	Square or almost square	Rectangular	Long rectangle	Complex (L, T, X, or geometry building shapes)
Building maintenance (pc)	Very good	Good	Average	Bad	Very bad

Table 2. Assessment of surrounding protection components [22,24]

Components	-1	-0.5	0	+0.5	+1
Building row	More than 10	7-10	4-6	2-3	1
Natural barrier	Very high protection	High protection	Average protection	Medium protection	No protection
Seawall height and shape	Vertical shape and seawall height is more than 5 m	Vertical shape and seawall height 3-5 m	Vertical shape and seawall height 1.5-3 m	Vertical with a height of 0-1.5 m or inclined with a height of 1.5-3 m	Sloping 0-1.5 m high or no seawall
Brick walls around the building	Wall height 80%-100% of water depth	Wall height 60%-80% of water depth	Wall height 40%-60% of water depth	Wall height 20%-40% of water depth	Wall height 0%-20% of water depth
moving object	Very low risk to moving objects		Average risk to moving objects		Very high risk from moving objects

One of the building resilience factors can be determined by water contact with the floor when an intrusion occurs. This intrusion can affect the vulnerability of a building. To determine the WV component score, we need to build a tsunami inundation model first (equation 6) [27].

$$WV = \frac{Inundation\ height}{Number\ of\ floors\ of\ the\ building} \qquad (6)$$

The modeling can be undertaken using ArcMap 10.8.1 software with a tsunami runoff height of 5 m. This tsunami runoff height is according to [28,29]. The maximum run-up height of the 2006

tsunami at Ayah Beach is 2.7–3 meters, and 3–3.8 meters for Widarapayung Beach. Therefore, a height of 5 meters is considered optimal to facilitate the classification of tsunami heights. Calculation of the area inundated by the tsunami is obtained according to mathematical calculations carried out by Berryman (2006), taking into account the analysis of the tsunami height loss per 1 meter of inundation distance, the slope, and surface roughness (equation 7) [30]. The tsunami inundation model flowchart follows in **Figure 1**:

$$H_{loss} = \left(\frac{167\, n^2}{H_o{}^{1/3}}\right) + 5\, Sin\,(S) \qquad (7)$$

Where:
H_{loss} = Loss of tsunami height per 1 m inundation distance (m)
n = Surface roughness coefficient
H_0 = The tsunami wave height at the coastline (m)
S = Slope (degree)

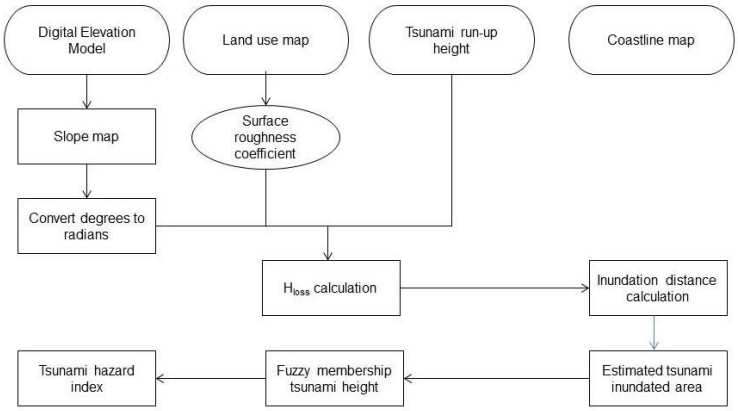

Figure 1. Flowchart of tsunami inundation modeling.

3. Results

The classification of tsunami inundation is divided into five classes, namely at a depth of 4-5 m, 3-4 m, 2-3 m, 1-2 m, and 0-1 m (**Table 3**). The Jetis beach is directly adjacent to the Kebumen District in the east with Gombong hills karst morphology. We estimate the tsunami inundation direction towards the west due to the difference in elevation between Kebumen, which has an alluvial plain morphology, and the Jetis Village has a low elevation and a slight difference from sea level. This elevation is a natural barrier that blocks tsunami waves to the east and drives tsunami direction westward.

Table 3. Classification of tsunami inundation

Class	Run-up height (m)	Area (hm^2)	Area (%)
1	Water body	9.44	16.34
2	0-1	12.68	16.31
3	1-2	12.66	12.07
4	2-3	9.37	9.38
5	3-4	7.28	33.73
6	4-5	26.18	12.16
Total		77.61	100

The vulnerability of buildings based on the PTVA–4 modeling resulted in several scores. The structural assessment of the building (SV) is obtained from the product of the three components of the assessment, namely, the value of the building's vulnerability (BV) (**Figure 2a**), the level of surrounding protection (Surr) (**Figure 2b**), and building exposure (Ex) (**Figure 2c**). The BV assessment score considered the number of floors (s), building materials and construction techniques (m), hydrodynamics of the ground floor (g), foundations (f), the building footprint shape (sh), and building maintenance (pc) parameters produces an interval score between 1 .03-5.45 which is categorized into three classes, namely Low (1.03-1.82), Medium (1.83-3.94), and High (3.95-5.45) (**Figure 2a**). The assessment of building protection (Surr) is based on the protection provided to the building by its surroundings in the form of a row of buildings (br), the presence of a seawall (sw), natural barriers (nb), the presence of a brick wall around the building (w), and the risk to a moving object (mo). Surr values range from 0.78-5.17, which are categorized into 3 classes, namely, Low (0.78-2.16), Medium (2.17 - 3.57), High (3.58 - 5.17) (**Figure 2b**). Exposure (Ex) is related to the depth of water flow at the measurement point. The degree of structural damage increases as the water depth rise because of the pressure exerted on the building. The flow velocity is a direct function of the flow depth. Exposure values at locations ranged from 1.00-2.54 (**Figure 2c**)

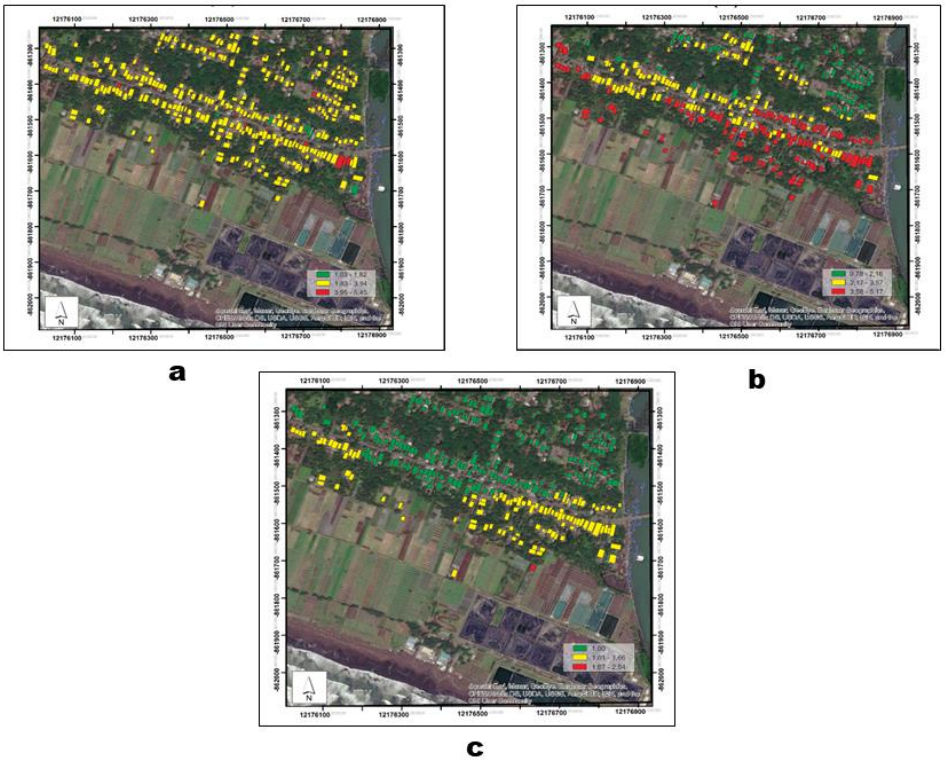

Figure 2. **(a)** Distribution of building vulnerability values (BV), **(b)** distribution of building protection values (Surr), **(c)** distribution of exposure values (Ex)

4. Discussion

The SV value is obtained by multiplying the three components (BV, Surr, and Ex), then simplified into three parts to categorize the results, with the values ranging from 1.00 to 3.87 (**Figure 3a**).

The assessment is influenced by the condition of each building and the effect on water intrusion so that buildings closer to the sea have a large enough vulnerability value. Based on the above analysis results, the SV value is divided into three parts, with each part representing its respective color, namely, for values with an interval of 1.00-1.84 (green) having low susceptibility, the value is 1.85-2.97 (yellow) has a moderate vulnerability, and a value of 2.98-3.30 (red) has a high vulnerability. The WV score is calculated based on the number of floors in the building divided by the number of flooded floors. The score also considers the contact with water which can affect the structural vulnerability of the building. Most of the scattered buildings consist of 1-story buildings. Therefore the difference in WV values is based on the distance between the buildings and the shoreline (**Figure 3b**). Buildings that have a low WV value (green) with a scale value of 1.00-1.99 are less risky than buildings with a higher WV value of 2.00-2.99 (yellow) and with a value above 3.00 (red). The assessment of the Relative Vulnerability Index (RVI) inputs two parameters, namely Structure Vulnerability (SV) and Wave Vulnerability (WV), into the formula to obtain values with an interval of 1.00-3.24 (**Figure 3c**). There are three categories of vulnerability in this case, low, medium, and high vulnerable (**Figure 3d**).

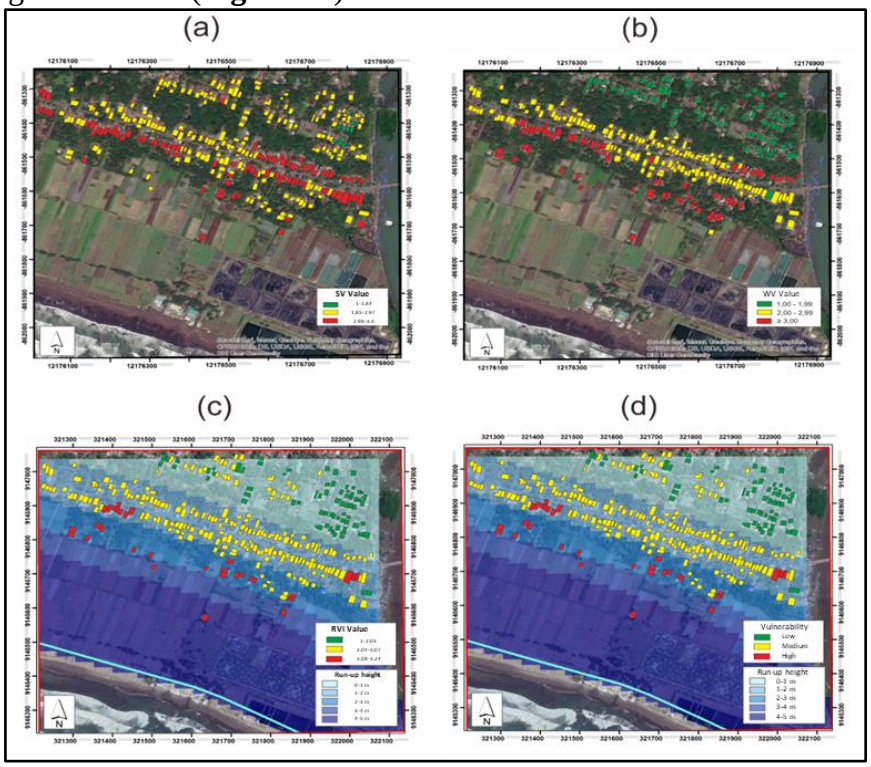

Figure 3. **(a)** Map of SV value distribution, **(b)** WV values distribution, **(c)** map of RVI value distribution, **(d)** Tsunami vulnerability map.

There are 69 buildings categorized as buildings with Low vulnerability risk (1.00-2.03), 169 buildings with Medium vulnerability risk (2.04-3.07), and 31 buildings with High vulnerability risk (3.08-3.21) (**Figure 4**).

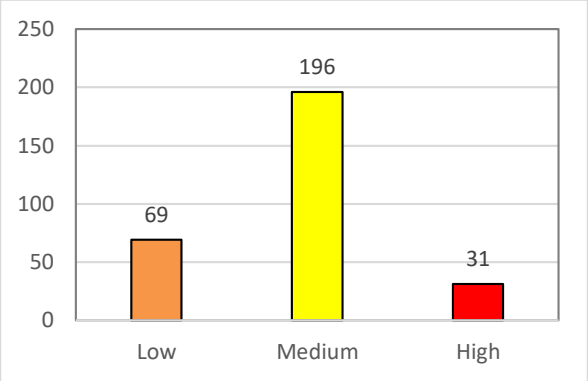

Figure 4. The number of building vulnerabilities graph

According to the PTVA–4 model, 296 existing building objects are vulnerable to tsunami hazards. Most of the buildings are situated about 540 meters from the shoreline. This distance is considered quite close to the tsunami risk area. The assessed building materials consist of temporary buildings made of wood and have a very shallow foundation and old buildings made of brick and more than 20 years old (**Figure 5**). The distance between buildings is relatively close. This factor can cause damage to buildings during a tsunami. The most influential factor in building damage when tsunami waves strike an area is the distance to the shoreline. Buildings located further away from the shoreline have a lower Relative Vulnerability Index (RVI) value, and automatically the risk experienced by these buildings is also lower. Based on the PTVA–4 model with an inundation height of 5 meters, it can be seen that all buildings in the Jetis are inundated with water, although at different heights. Most buildings 500 meters from the shoreline were submerged to 1-2 meters.

Figure 5. List of buildings in Jetis, **(a)** mosque, **(b)** residents' houses, **(c)** stores, **(d)** temporary buildings.

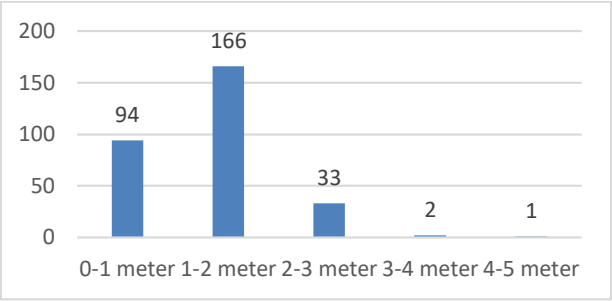

Figure 6. The number of inundated buildings per class

Figure 6 reveals that one building will be submerged in water with a 4-5 m. Most buildings will only sink 1-2 m in the event of a tsunami. The absence of a seawall in Jetis causes the vulnerability of the building to be high. Seawalls help reduce the power of the tsunami so that the inundation of populated areas can be minimized. Natural barriers such as trees that are high enough can block the tsunami flow. Several optional solutions can be made in applying building vulnerability values, including relocation of residential areas with high vulnerability. Sites with a low level of inundation (0-1 meters) can be made on two floors to minimise losses. Extensive tree planting can be a natural barrier to reducing the tsunami's strength. Structured Seawall Creation should be considered as an option.

Conclusions

The building vulnerability index modelling using PTVA–4 is easy to apply and has high reliability, as evidenced by the modelling results that are close to the actual conditions in the 2006 building vulnerability index study in Cilacap, Central Java. There are 296 tsunami-prone buildings with a distance of 540 m from the shoreline based on PTVA–4 modelling with a run-up of 5 m. In the 2006 tsunami on the south coast of Cilacap, 296 buildings were seriously damaged. In addition, this method can be applied to a preliminary study of tsunami-prone zones and local authorities with limited technology and funds for disaster management.

References

[1] Suppasri A, Muhari A, Syamsidik, Yunus R, Pakoksung K, Imamura F, Koshimura S, Paulik R. Vulnerability characteristics of tsunamis in indonesia: analysis of the global centre for disaster statistics database. Journal of Disaster Research 2018;13:1039-1048.

[2] Pilarczyk JE, Dura T, Horton BP, Engelhart SE, Kemp AC, Sawai Y. Microfossils from coastal environments as indicators of paleo-earthquakes, tsunamis and storms. Palaeogeography Palaeoclimatology Palaeoecology 2014; 413:144-157.

[3] Laksono FAT, Tsai LLY, Pilarczyk J. The sedimentological record of Upper Holocene tsunami event in Fengbin, Taiwan. Geopersia 2021; 11:169–203.

[4] Fujii Y, Satake K. Source of the July 2006 West Java tsunami estimated from tide gauge records. Geophysical Research Letters 2006; 33: 1-5.

[5] Gunawan E, Meilano I, Abidin H Z, Hanifa NR, Susilo. Investigation of the best coseismic fault model of the 2006 Java tsunami earthquake based on mechanisms of postseismic

deformation. Journal of Asian Earth Sciences 2016; 117:64-72.
[6] Samaras AG, Karambas TV, Archetti R. Simulation of tsunami generation, propagation and coastal inundation in the Eastern Mediterranean. Ocean Science 2015; 11:643-655.
[7] Tappin DR. Submarine landslides and their tsunami hazard. Annual Review of Earth and Planetary Sciences 2021; 49:551-578.
[8] Rosalia S, Widiyantoro S, Nugraha AD, Supendi P. Double-difference tomography of p-and s-wave velocity structure beneath the western part of Java, Indonesia. Earthquake Science 2019; 32:12-25.
[9] Sassa S, Takagawa T. Liquefied gravity flow-induced tsunami: first evidence and comparison from the 2018 Indonesia Sulawesi earthquake and tsunami disasters. landslides 2019; 16: 195-200.
[10] Shinozaki T, Sawai Y, Hara J, Ikehara M, Matsumoto D, Tanigawa K. Geochemical characteristics of deposits from the 2011 Tohoku-oki tsunami at Hasunuma, Kujukuri coastal plain, Japan. Island Arc 2016; 25: 350–368.
[11] Macías J, Castro MJ, Ortega S, González-Vida JM. Performance assessment of Tsunami-HySEA model for NTHMP tsunami currents benchmarking. Field cases. Ocean Modelling 2020; 152:101645.
[12] Strusińska-Correia A. Tsunami mitigation in Japan after the 2011 Tōhoku Tsunami. International Journal of Disaster Risk Reduction 2017; 22: 397-411.
[13] Salmanidou DM, Ehara A, Himaz R, Heidarzadeh M, Guillas S. Impact of future tsunamis from the Java trench on household welfare: Merging geophysics and economics through catastrophe modelling. International Journal of Disaster Risk Reduction 2021; 61:102291.
[14] Dewi RS. A-GIS based approach of an evacuation model for tsunami risk reduction. Journal of Integrated Disaster Risk Management 2012; 2:108-39.
[15] Asri AK, Elya H, Duantari N, Suryaningsih E, Victoria LDDD. Dual mitigation system: database system combination of EWS and APRS for disaster management (case study: Malang southern coast). Procedia - Social and Behavioral Sciences 2016; 227:435-441.
[16] Kato T, Ito T, Abidin HZ, Agustan. Preliminary report on crustal deformation surveys and tsunami measurements caused by the July 17, 2006 south off Java island earthquake and tsunami, Indonesia. Earth, Planets and Space 2007; 59: 1055-1059.
[17] Hall S, Pettersson J, Meservy W, Harris R, Agustinawati D, Olson J, McFarlane A. Awareness of tsunami natural warning signs and intended evacuation behaviors in Java, Indonesia. Natural Hazards 2017; 89:473-496.
[18] Koulali A, McClusky S, Susilo S, Leonard Y, Cummins P, Tregoning P, Meilano I, Efendi J, Wijanarto AB. The kinematics of crustal deformation in Java from GPS observations: Implications for fault slip partitioning. Earth and Planetary Science Letters 2017; 458:69-79.
[19] Mardiatno D, Malawani MN, Nisaa' RM. The future tsunami risk potential as a consequence of building development in Pangandaran Region, West Java, Indonesia. International Journal of Disaster Risk Reduction 2020; 46:101523.
[20] Widiyantoro, S., Gunawan, E., Muhari, A., Rawlinson, N., Mori, J., Hanifa, N. R., Susilo, S., Supendi, P., Shiddiqi, H. A., Nugraha, A. D., and Putra, H. E. (2020). Implications for megathrust earthquakes and tsunamis from seismic gaps south of Java Indonesia. *Sci Rep* 2020; 10:15274.
[21] Abdurrachman M, Widiyantoro S, Priadi B, Alim MZA, Dewangga AH. Proposed new

wadati-benioff zone model in Java-Sumatra subduction zone and its tectonic implication. Joint Convention Balikpapan 2015; 1: 1-4.
[22] Izquierdo T, Fritis E, Abad M. Analysis and validation of the PTVA tsunami building vulnerability model using the 2015 Chile post-tsunami damage data in Coquimbo and la Serena cities. Nat Hazards Earth Syst Sci 2018; 18:1703-1716.
[23] Dall'Osso F, Dominey-Howes D, Tarbotton C, Summerhayes S, Withycombe G. Revision and improvement of the PTVA-3 model for assessing tsunami building vulnerability using "international expert judgment": introducing the PTVA–4 model. Natural Hazards 2016; 83:1229-1256.
[24] Papathoma-Köhle M, Cristofari G, Wenk M, Fuchs S. The importance of indicator weights for vulnerability indices and implications for decision making in disaster management. International Journal of Disaster Risk Reduction 2019; 36:101103.
[25] Batzakis DV, Misthos LM, Voulgaris G, Tsanakas K, Andreou M, Tsodoulos I, Karymbalis E. Assessment of building vulnerability to tsunami hazard in kamari (Santorini island, greece). J Mar Sci Eng 2020; 8:886.
[26] Harisuthan S, Hasalanka H, Kularatne D, Siriwardana, C. Applicability of the PTVA–4 model to evaluate the structural vulnerability of hospitals in Sri Lanka against tsunami. International Journal of Disaster Resilience in the Built Environment 2020; 11:581-596.
[27] Madani S, Khaleghi S, Jannat MRA. Assessing building vulnerability to tsunami using the PTVA-3 model: a case study of Chabahar Bay, Iran. Natural Hazards 2017; 85:349-359.
[28] Aditama MR, Sunan HL, Laksono FAT, Ramadhan G, Iswahyudi S, Fadlin. Integrated Subsurface Analysis of Thickness and Density for Liquefaction Hazard: Case Study of South Cilacap Region, Indonesia. Journal of Geoscience, Engineering, Environment, and Technology 2021; 6:58-66.
[29] Laksono FAT, Widagdo A, Aditama MR, Fauzan MR, Kovács J. Tsunami hazard zone and multiple scenarios of tsunami evacuation route at Jetis Beach, Cilacap Regency, Indonesia. *Sustain* 2022; 14:2726.
[30] Tarbotton C, Dominey-Howes D, Goff JR, Papathoma-Kohle M, Dall'osso F, Turner IL. GIS-based techniques for assessing the vulnerability of buildings to tsunami: Current approaches and future steps. Geological Society Special Publication 2012; 361:115.